

# The ISO spectrum of the planetary nebula NGC 6302

## II. Nebular abundances

S.R. Pottasch<sup>1</sup> and D.A. Beintema<sup>2</sup>

<sup>1</sup> Kapteyn Astronomical Institute, P.O. Box 800, 9700 AV Groningen, The Netherlands

<sup>2</sup> SRON Laboratory for Space Research, P.O. Box 800, 9700 AV Groningen, The Netherlands

Received 2 February 1999 / Accepted 9 April 1999

**Abstract.** The ISO spectrum of NGC 6302 is used, in conjunction with the visible and ultraviolet spectrum, to determine the nebular composition. In addition to being considerably more accurate than previous determinations, the abundances of many more elements (and ions) can be found. A discussion of the previous evolution of the central star, in the light of these abundances, is given. A discussion is also given of the composition of the dust.

**Key words:** stars: abundances – stars: evolution – ISM: planetary nebulae: individual: NGC 6302 – infrared: ISM: lines and bands

### 1. Introduction

Nebular abundances are the most important information for determining the evolution of the central star. As such, they have been studied for many years. The accuracy of the abundance is hard to judge. Aller (1994) estimates the uncertainty as about a factor of 2, but he may be optimistic. As pointed out by Pottasch (1997), a comparison of the most recent abundance determinations for the 5 most abundant elements in the bright planetary nebulae NGC 7027, gives reason for concern. Of the 4 determinations made since 1990, there is a factor of 3 difference between the highest and lowest value for nitrogen, oxygen and neon, and a factor of 6 difference for carbon and magnesium.

It is not clear what the problem is. It probably has to do with the following:

1. uncertainties in the electron temperature, or temperature fluctuations in the nebula.
2. different ways of correcting for the unseen stages of ionization.
3. different corrections for the extinction to, or within, the nebula.
4. uncertainties in the electron density, or density fluctuations in the nebula.
5. uncertainties in the atomic parameters, especially the cross-section for electron collisional excitation.

*Send offprint requests to:* pottasch@astro.rug.nl

The use of the ISO infrared spectrum removes or alleviates several of these problems. Concerning (1) the infrared lines originate from levels so close to the ground level that the electron temperature does not enter in an important way in populating these levels. Concerning (2), so many additional ions are observed in the infrared that, as will be shown below, the uncertainty of the correction for unseen ionization stages is much reduced. The correction for extinction (3) is negligible in most of the ISO range and small in the near infrared. The electron density (4) is usually unimportant in the probable range, but there are cases which require a careful discussion of the density. Finally, new values of collisional cross-sections have become available in the past several years which reduce the uncertainty in the atomic data (the IRON project). The absolute uncertainty in the atomic data, may still be occasionally large.

The ISO spectrum of NGC 6302 for a large region in the central part of the nebula has been presented and discussed in a previous paper (Beintema & Pottasch, 1999, hereafter Paper I). The optical and ultraviolet spectrum in essentially the same part of the nebula has also been presented. In this paper it is intended to use this spectrum to derive the element abundances. In Sect. 2 we will discuss the method to be followed. In Sect. 3 the nebular density and temperature in the region observed. In Sect. 4 the ionic abundances will be given, together with the total element abundances. These results will be discussed in Sect. 5.

### 2. Method of analysis

NGC 6302 as seen in the optical is somewhat irregular, elongated, and is crossed near the center by a dark dust lane. At very low intensity levels a large bi-lobal structure is seen. Our spectra (Paper I) are confined to the central  $14 \times 20$  arcsec where the bi-lobal structure is unimportant. The radio map (see Paper I) shows no important structures in this region of peak intensity. There is no evidence for a shell structure.

For this reason, we shall assume, as a first approximation, that the spectrum is coming from a region of constant density and temperature. This can then be checked. For example, there are 10 ions where measured line ratios are dependent almost entirely on the electron density,  $N_e$ . These ions have a variety of ionization potentials, ranging from 10.4eV (S II) to 97eV (Ne V).

**Table 1.** Electron density indicators

Ion	Ioniz. Pot.	Lines used	Observed ratio	Electron density	Ref
S II	10.4	6731/6716	2.00±0.04	10800±1500	2
O II	13.6	3726/3729	2.17±0.01	8100±300	2
S III	23	33.5/18.7	0.35±0.04	5000±600	1
Cl III	24	5538/5518	2.4±0.2	23000±5000	3
C III	24	1907/1909	1.1±0.1	17000±1000	2
Ar III	28	21.8/8.99	0.059	<18000	1
Ar IV	40.7	4740/4711	1.79±0.03	14500±500	2
Ne III	41	15.5/36.0	16.2±1.7	20000±15000	1
Ar V	60	13.1/7.9	1.5±0.15	3000±2500	1
Ne V	97	24.3/14.3	0.49±0.05	10000±1500	1

References: (1) Paper I, (2) Barral et al. 1982, (3) Oliva et al. 1996.

It is expected that the ions with higher ionization potential will be formed closer to the central star. If the derived densities vary as a function of ionization potential of the observed ion, it is an indication that the density varies with the position in the nebula. If necessary, this can then be used to refine the model.

It is assumed that the ions considered are in statistical equilibrium and can be represented by the lowest 5 levels. The collisional excitation is assumed to occur by electron collisions, where the cross-sections used are all from the recent publications of the “IRON project”. The individual references can be found in

<http://www.am.qub.ac.uk/projects/iron/papers/papers.html>.

The Einstein A values are either summarized by Mendoza (1983), or a reference is given there where they can be found.

### 3. Electron density

The ions from which line ratio's can be used to determine  $N_e$  are listed in the first column of Table 1. The ionization potential required to reach that ionization stage is in Column 2. The wavelengths of the lines used are given in the third column, where the units are Å when 4 ciphers are given and microns when 3 ciphers are given. The observed ratio of these lines is given in the fourth column, where the errors are those given by the observers. For the ISO data, we estimate a 10% error ( $1\sigma$ ) for the ratio. The derived value of  $N_e$  for a value of  $T_e = 18000$  K is given in Column 5, together with the  $1\sigma$  uncertainty. The reference for the observed ratio is given in the last column.

The ratio given for the Ar III lines is a lower limit because the  $8.99\mu\text{m}$  line is a blend of Ar III with Mg VII. The Ne III density has a large uncertainty because the line ratio is not very sensitive to the density at values of  $N_e \sim 10^4\text{ cm}^{-3}$ .

The choice of  $T_e = 18000$  K is justified in the following section. However, the density value given is insensitive to the precise value and the error given covers  $15000\text{ K} \leq T_e \leq 20000\text{ K}$ . The uncertainty in the collisional excitation rates is not included in the error, because it is not known.

On examining the values of  $N_e$  in the table there is no indication that a systematic trend with ionization potential exists. Within a factor 2, all values are consistent with the weighted

mean of  $N_e = 11000\text{ cm}^{-3}$ . The factor 2 can simply be caused by the fact that the observational errors are actually sometimes greater than the 10% estimated, coupled with the fact that  $N_e$  is sometimes a non-linear function of the observed ratio. In addition there is a further error caused by the uncertainty in the atomic parameters. This error is very hard to quantify because it depends on how sensitive the ratio is to the density. The calculations of the collision strengths include its variation with electron temperature. The variation is usually not large and may either increase or decrease with temperature, depending on the ion.

It is interesting to compare this value of density with the rms density found from the strength of the  $H\beta$  line. This depends on the distance and for this calculation  $d = 1.6$  Kpc is used (Terzian, 1997). It is assumed that  $N_p = 0.8 N_e$ , and that the observed  $H\beta$  emission originates in a sphere of 16 arc sec diameter, which is a reasonable approximation to the aperture used in Paper I. The rms density is:

$$\langle N_e \rangle_{rms} = 11000\text{ cm}^{-3}$$

which is in good agreement with the individual values in Table 1. This indicates that there are no large scale densities inhomogeneities in the nebula.

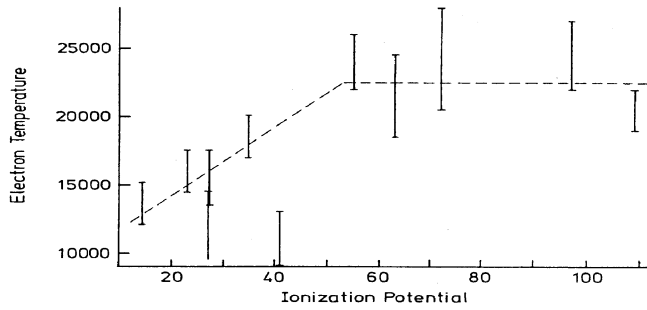
In the rest of this paper we will use the value  $N_e = 11000\text{ cm}^{-3}$ , constant over the emitting region of the aperture.

### 4. Electron temperature

In the visual spectra two ions are available which have lines originating from levels of sufficiently different energy so that the ratio can be used to determine the electron temperature  $T_e$ . These are O III and N II. When the SWS infrared lines are included, at least 9 other ions become available, although a few of these lines also have a density dependence. These ions are listed in the first column of Table 2; the ionization potential of the lower stage of ionization is given in Column 2. The line ratio used to determine the temperature is given in Column 3. When other lines of the same ion are available they usually give the same temperature. In the single case where a difference exists, Ar III, the temperature resulting from two different line ratio's is given. The observed line ratio, with the estimated  $1\sigma$  error, is given in Column 4, and the resulting value of  $T_e$ , with its error, is given in Column 5. In those cases in which an electron density was also necessary, the value determined in the previous section was used. There appears to be a relationship between  $T_e$  and the ionization potential. This is also shown in Fig. 1. The higher temperatures are found from the ions with the higher ionization potential. Above an ionization potential of  $50\text{ eV}$  the temperature appears to remain constant at a value  $T_e \sim 22000$  K. Below  $40\text{ eV}$  the temperature drops, reaching its lowest value of about  $14000$  K for N II. Since the ions with high ionization potential are formed closer to the central star, it appears that the temperature in the central regions is, as expected, the highest, and it decreases toward the outer regions. It is rather difficult to specify this more quantitatively since (1) the exact position of the aperture is uncertain within  $\pm 3''$ , (2) the spectrum is integrated

**Table 2.** Electron temperature indicators

Ion	Ioniz. Pot.	Lines used	Observed ratio	Electron temp.
N II	14.5	5755/6584	0.040±0.0008	13600±1500
S III	23.3	6312/18.7	0.19±0.02	16000±1500
Ar III	27.6	5192/21.8	0.40±0.1	13500±2500
Ar III	27.6	5192/7136	0.195±0.03	15500±2000
O III	35	4363/5007	0.0306±0.003	18500±1500
Ne III	41	3868/15.5	0.61±0.1	11000±2000
O IV	55	1400/25.9	1.25±0.3	23000±2000
Ne IV	63	2425/4725	61.5±6.2	21500±3000
Na IV	72	3242/9.04	2.9±0.6	25000±5000
Ne V	97	3426/14.3	1.11±0.2	24500±2500
Mg V	109	2783/5.61	0.89±0.1	20000±1500

**Fig. 1.** The electron temperature as determined from different ions is plotted as a function of the ionization potential of the ion. The ions are specified in Table 2.

along the line of sight, and (3) the original IR, optical and UV spectral lines may not refer to precisely the same spatial regions in the nebula. Although an effort was made in the reduction for them to be consistent with each other within a common area, some residual differences may have remained.

As can be seen from the table and figure, the Ne III ion gives a value of  $T_e$  considerably lower than given by the other ions. Although there is only one measurement of the  $\lambda$  3868 line in the literature (Aller et al. 1981), it is unlikely that the line strength is so far wrong (to obtain  $T_e = 20\,000$  the  $\lambda$  3868 line would have to be 5 times stronger). It is possible that the electron collision cross-sections are overestimated, but the IRON project values are estimated to be correct to within 10% (Butler & Zeppen 1994). The O IV temperature is calculated on the assumption that the  $\lambda$  1400 Å line is mainly O IV and that Si IV is only a minor contributor. If Si IV were an important contributor, the temperature would be lower.

The precise value of the temperature is not of great importance for determining the abundance of ions which emit fine structure lines in the infrared. This is the majority of the ions. For ions which are represented only by lines in the visual or ultraviolet, the temperature used will depend on the ionization potential as shown by the dashed line in Fig. 1. The error in the abundance of these ions will consequently be somewhat greater.

Since the hydrogen lines are formed over the entire region an average temperature should be used. This average should be

weighed according to the amount of material at a given temperature. Since this is difficult to calculate without discussing the stellar spectrum and the geometry of the emitting gas, we have chosen to use the value  $T_e = 18\,000$  K for the hydrogen spectrum. Since the actual average value is certainly between 16 000 K and 20 000 K, and the error introduced depends only on the square root of the temperature, the resultant uncertainty is only 5 or 6%. This is smaller than the errors of measurement.

## 5. Ionic abundances

The ionic abundances have been determined using the following equation:

$$\frac{N_{ion}}{N_p} = \frac{I_{ion}}{I_{H\beta}} N_e \frac{\lambda_{ul}}{\lambda_{H\beta}} \frac{\alpha_{H\beta}}{A_{ul}} \left( \frac{N_u}{N_{ion}} \right)^{-1} \quad (1)$$

where  $I_{ion}/I_{H\beta}$  is the measured intensity of the ionic line, originating from level  $u$  in the ion, compared to  $H\beta$ ;  $N_p$  is the density of (ionized) hydrogen;  $\lambda_{ul}$  is the wavelength of this line and  $\lambda_{H\beta}$  is the wavelength of  $H\beta$ ;  $\alpha_{H\beta}$  is the effective recombination coefficient for  $H\beta$ ;  $A_{ul}$  is the Einstein spontaneous transition rate for the line, while  $N_u/N_{ion}$  is the ratio of the population of the level from which the line originates to the total population of the ion. This ratio has been determined using the 5 level atom described above. The results are given in Table 3. The first column lists the ion concerned. The second column gives the wavelength of the line (or lines) used to determine the ionic abundance (relative to hydrogen). The intensity of that line is taken from Paper I. It is interesting to note that (excluding helium) an infrared line was used for 41 of the 57 ions listed. This means that most ionic abundances (listed in Column 3 of the table) are not sensitive to the electron temperature nor to the possibility of electron temperature fluctuations. Only C, N and to some extent O, are temperature dependent. When the ion is temperature dependent, the temperature used is that discussed in the previous section. In addition the ionic abundance is usually insensitive to the electron density. Only in those cases where the  $A$  value for the transition is smaller than  $10^{-3} \text{ sec}^{-1}$  is there an important  $N_e$  dependence (Si II and O IV). Even in these cases the dependence varies linearly with the density, i.e. there is no exponential dependence.

The fourth column gives the sum of the observed ions of a given element. The fifth and sixth columns give the ionization correction factor (ICF) and the total abundance of each element (relative to hydrogen). These were calculated on a purely empirical basis, in the following manner. First it was noted that the maximum ionic abundance occurs for ions which require 30 to 50  $ev$  to be produced. For ions with higher ionization potentials the ionic abundance slowly decreases. From the magnesium and silicon ions, it can be seen that above ionization potentials of 200 to 240  $ev$  the ionic abundance becomes very small and for our purposes these ions contribute very little to the element abundance. As an example consider the case of neon. All of the abundant ions are seen. On the high ionization side a small contribution may be found in Ne VII and Ne VIII. Judging from the rather rapid decline from Ne III through Ne VI, it is unlikely that

**Table 3.** Ionic concentrations and chemical abundances. Wavelength in Angstrom for all values of  $\lambda$  above 1 000, otherwise in  $\mu\text{m}$ .

Ion	$\lambda$	$n(\text{ion})/n_p$	$\Sigma n(\text{ion})/n_p$	ICF	$n(\text{element})/n_p$
He <sup>+</sup>	4472	0.11			
He <sup>++</sup>	4686	0.061	0.17		0.17
C <sup>++</sup>	1909	2.2(-5)			
C <sup>+3</sup>	1548	1.4(-5)	3.7(-5)	1.68	6.0(-5)
N <sup>+</sup>	6584	2.9(-5)			
N <sup>++</sup>	1750	6.8(-5)			
N <sup>+3</sup>	1487	7.8(-5)			
N <sup>+4</sup>	1238	6.4(-5)	2.4(-4)	1.2	2.9(-4)
O <sup>0</sup>		1.1(-5)			
O <sup>+</sup>	3727	1.1(-5)			
O <sup>++</sup>	5007	9.0(-5)			
O <sup>+3</sup>	25.9	5.9(-5)	1.71(-4)	1.35	2.3(-4)
Ne <sup>+</sup>	12.8	5.2(-5)			
Ne <sup>++</sup>	15.55	7.8(-5)			
Ne <sup>+3</sup>	2425	3.5(-5)			
Ne <sup>+4</sup>	14.3,24.3	2.2(-5)			
Ne <sup>+5</sup>	7.65	7.0(-6)	1.95(-4)	1.1	2.2(-4)
Na <sup>++</sup>	7.31	6.0(-7)			
Na <sup>+3</sup>	9.038,3242	2.5(-7)			
Na <sup>+5</sup>	8.607,14.39	6.4(-7)			
Na <sup>+6</sup>	4.68	2.1(-7)	1.7(-6)	1.5	2.6(-6)
Mg <sup>+3</sup>	4.49	1.3(-6)			
Mg <sup>+4</sup>	5.61,13.51	4.4(-6)			
Mg <sup>+6</sup>	5.50	1.51(-6)			
Mg <sup>+7</sup>	3.03	3.8(-8)	7.24(-6)	1.8	1.3(-5)
Al <sup>+4</sup>	2.91	<1.8(-9)			
Al <sup>+5</sup>	3.66,9.11	2.8(-9)			
Al <sup>+7</sup>	3.69	1.4(-9)	4.2(-9)	2.4	1.0(-8)
Si <sup>+</sup>	34.8	6.8(-6)			
Si <sup>++</sup>	1892	1.0(-6)			
Si <sup>+5</sup>		3.5(-6)			
Si <sup>+6</sup>	2.48,6.49	2.1(-6)			
Si <sup>+8</sup>	3.94	1.8(-9)	1.34(-5)	1.7	2.3(-5)
S <sup>+</sup>	6731	1.3(-6)			
S <sup>++</sup>	18.7,33.5	2.2(-6)			
S <sup>+3</sup>	10.5	1.3(-6)			
S <sup>+7</sup>	9918	3.8(-7)	5.2(-6)	1.5	7.8(-6)
Cl <sup>+</sup>	14.36,8577	7.2(-8)			
Cl <sup>++</sup>	5538	3.7(-8)			
Cl <sup>+3</sup>	11.76	2.1(-8)			
Cl <sup>+4</sup>	6.70	7.9(-8)	2.1(-7)	1.65	3.4(-7)
Ar <sup>+</sup>	6.99	1.5(-6)			
Ar <sup>++</sup>	21.8,7137	2.0(-6)			
Ar <sup>+3</sup>	4740	8.6(-7)			
Ar <sup>+4</sup>	13.10,7.90	3.6(-7)			
Ar <sup>+5</sup>	4.54	4.1(-7)	5.1(-6)	1.2	6.0(-6)
K <sup>++</sup>	4.62	3.0(-8)			
K <sup>+3</sup>	5.98	1.9(-8)			
K <sup>+5</sup>	5.58,8.83	1.1(-8)			
K <sup>+6</sup>	3.19	3.3(-9)	6.3(-8)	1.35	8.5(-8)
Ca <sup>+3</sup>	3.207	1.3(-8)			
Ca <sup>+4</sup>	4.16	2.5(-8)			
Ca <sup>+6</sup>	4.08	3.0(-9)			
Ca <sup>+7</sup>	2.32	1.8(-10)	4.1(-8)	1.8	7.4(-8)
Fe <sup>+</sup>	25.98	2.1(-7)			
Fe <sup>++</sup>	22.9	≤1.0(-7)			

**Table 3.** (continued)

Ion	$\lambda$	$n(\text{ion})/n_p$	$\Sigma n(\text{ion})/n_p$	ICF	$n(\text{element})/n_p$
Fe <sup>+3</sup>		≤2.1(-7)			
Fe <sup>+4</sup>	20.8	3.0(-8)			
Fe <sup>+5</sup>	14.8,19.6	2.0(-7)			
Fe <sup>+6</sup>	9.52	6.0(-8)	7.2(-7)	1.2	8.7(-7)

more than 5 to 8% of the neon is in the two unseen ionization stages. A more difficult problem is whether any neutral neon is present, since its ionization potential of 21.6 *ev* would allow its presence in the ionized hydrogen region. But if it is present, the amount is not substantial, since even the amount of singly ionized neon is considerably less than that of doubly ionized neon. We have thus increased the total amount of neon to be 10% more than the total of the observed neon ions, or an ICF of 1.1. As can be seen from Table 3, the ICF is almost always less than 1.8, which is a rather small uncertainty. This reflects the fact that usually very many of the important ionization stages are seen. Only in the case of aluminium is the estimated ICF higher; this is because no lines originating from the 4 lowest ionization stages have been seen.

An estimate of the possible error in the element abundance is rather difficult to give, because it depends not only on accuracy of the measured line strengths, the ICF and occasionally on  $N_e$  and/or  $T_e$ , but also on the atomic parameters, especially the electron collision cross-section. Assuming that the estimate of the uncertainty of the latter is 10 to 20% as indicated by the IRON group papers, we estimate the total element uncertainty to be about 30%, sometimes a little less, sometimes a little more. The reason for such a low uncertainty is the fact that even a factor 2 uncertainty in a given ion will be moderated by the inclusion of other ions of the same element.

## 6. Comparison with other abundance determinations

The abundances found are summarized in the first two columns of Table 4. For comparison the results of Aller et al. (1981) are given in column 3. For some elements the agreement is good, but for others there is substantial disagreement. For Si and Ca the differences amount to more than a factor 3, but in both cases Aller et al. were only able to measure a single ionization state. When a comparison is made between individual ionization states it is seen that disagreements of a factor of 3 or 4 are not uncommon. But these are somewhat reduced when the total element abundances are compared. There are many reasons for these disagreements. First the collisional excitation cross-section may be different. For example, the N III cross-section is now thought to be a factor of 2 higher which reduces the N III abundance by the same factor. Secondly different measurements were used. For example, the O IV abundance was determined from the 25.9 micron lines, which has the effect of lowering the abundance by a factor 3. Similarly the Ne III abundance was determined from the strong infrared lines at 15.5 and 36.0 microns, causing an in-

**Table 4.** Comparison of abundances in NGC 6302 ( $\log(X/H) \times 12$ )

Element	Present Abundance	Aller et al. (1981)	Sun <sup>1</sup>	B Star <sup>2</sup>	ISM $\zeta$ Oph <sup>3</sup>	Orion <sup>4,5</sup>
Helium		11.26				
Carbon	7.78	8.00	8.55	8.24	8.14	8.49
Nitrogen	8.46	8.92	7.97	7.81	7.90	7.83
Oxygen	8.36	8.70	8.87	8.62	8.48	8.60
Neon	8.34	7.99	8.08	8.09		7.91
Sodium	6.42	6.57	6.31		5.36	
Magnesium	7.11		7.58	7.38	6.03	
Aluminium	4.00		6.48	6.37		
Silicon	7.36	6.9	7.55	7.38	6.24	6.65
Sulfur	6.90	6.80	7.27	7.09	7.45	6.97
Chlorine	5.53	5.59	5.27	5.27	5.08	
Argon	6.78	6.93	6.56		6.08	6.42
Potassium	4.93	5.32	5.13		4.04	
Calcium	4.87	5.36	6.34		2.61	
Iron	5.95		7.51	7.55	5.23	6.43

<sup>1</sup> Solar abundance from Grevesse & Noels (1993) and Anders & Grevesse (1989).

<sup>2</sup> B star abundance are the average of Gies & Lambert (1992) and Killian-Montenbruck et al. (1994) and have an uncertainty of 0.2 dex.

<sup>3</sup> ISM abundance in from Savage & Sembach (1996) and refers to the cool clouds in the direction of  $\zeta$  Oph. A typical uncertainty compared to other clouds is at least 0.2 dex.

<sup>4</sup> Rubin et al. (1991, 1993)

<sup>5</sup> Osterbrock et al. (1992)

crease of the abundance by almost a factor 4.<sup>1</sup> Thirdly, many of the abundances found by Aller et al. are dependent on  $T_e$  and/or  $N_e$ , for which somewhat different values were used than found here. For example they used  $N_e = 7\,200\text{ cm}^{-3}$ , somewhat lower than the value of  $11\,000\text{ cm}^{-3}$  discussed in Sect. 3. Finally, the large increase in the number of observed ionization stages can make a considerable difference in the total abundance, because it is often very difficult to account for missing ionization stages, especially when only one or two ionization stages of a given element are observed.

The carbon, nitrogen and oxygen abundances found here are somewhat lower than found by Aller et al., although the C/O and N/O ratios are similar. On the other hand, we find a higher neon abundance, which seems to be reliable, because all important ionization stages have been observed, and all but one are represented by ISO infrared lines. The neon abundance appears to be the same as oxygen, and in fact the total energy loss in the neon lines is comparable to that in the oxygen lines, confirming that this is a reasonable result.

Magnesium, aluminum and iron abundances are measured for the first time in this nebula. It is probably also the first time that reliable abundances for the latter two elements have been obtained in any nebula.

<sup>1</sup> The reason that the  $\lambda 3868\text{A}$  line gives a low abundance is something we cannot explain, but it is clearly related to the very low electron temperature obtained from this line.

## 7. Comparison with abundances in the Sun and B stars

In the study of evolution and the creation of the elements in PN, it is interesting to compare the abundances in this nebula with those in earlier evolution stages. In particular we can compare with solar abundances as an example of a middle-aged solar mass star, and with the B stars, which are younger, heavier stars; the latter are therefore more likely to be the foreloper of the central star of NGC 6302.

In Column 4 of Table 4 the solar abundances, taken from Anders & Grevesse (1989) and Grevesse & Noels (1993) are shown. The 5th column lists the B star abundances. These are the average of the values given by Gies & Lambert (1992) and Killian-Montenbruck et al. (1994). These two references sometimes differ by a factor 2 for a given element, which is a measure of the uncertainty of these abundances. The number of elements reported for the B stars is less than in the Sun or in NGC 6302.

When comparing the abundances in these objects, several things are noticeable. First, consider C, N and O. The ratio N/O is clearly larger in NGC 6302 than in the sun or B stars, in agreement with Aller et al. (1981). The ratio C/O  $\simeq 0.27$  is somewhat lower than in the sun but, within the uncertainties, the same as in B stars. The sum (C+N+O)/H is somewhat lower in NGC 6302 than in the sun, but about the same as in B stars. This has the consequence that it is possible that the central star of NGC 6302 evolved from a B star, and in the process converted some of its oxygen and carbon into nitrogen. Secondly, the abundance of neon and argon are somewhat higher in NGC 6302 than in the sun or B stars. The difference, a factor of about 1.7, is marginal. If it is true, it would mean that these elements are produced in the course of evolution.

The remainder of the elements can be divided into two groups: the first have abundances very similar to the sun and the B stars, and the second have substantially different abundances. The first group consists of Na, Si, S and Cl. The second group consists of Mg, Al, Ca and Fe. It is uncertain to which group K belongs. The accepted interpretation of the lower abundances is that these elements are “tied up” in the dust component which is abundantly present as the infrared bands attest to.

In this case it is strange that silicon does not belong to this group since the infrared bands indicate it is one of the most important components of the dust (Waters et al. 1996). However the error on the silicon abundance still allows an important amount to be present in dust. We shall discuss this further in the next section.

## 8. Comparison with abundances in the nearby interstellar medium

In the last two columns of Table 4, the abundances in the neighboring interstellar medium (ISM) are shown. Column 6 gives the abundance in the cool clouds in the direction of  $\zeta$  Oph, taken from Savage & Sembach (1996). These clouds are the ones which have been studied in the most detail, and are reasonably typical for cool clouds to within a factor 2. The last column gives the abundances in the Orion nebula, the brightest and nearest H II region. The abundances were taken from

**Table 5.** Outer regions of NGC 6302. Intensities  $10^{-12}$  erg cm $^{-2}$  s $^{-1}$ 

Line	$\lambda$	*Predict. Intens. Inner Reg.	Measur. Intens. LWS Tot.	Outer Reg. Intens.	Ion Abund.
O I	63	3.1	289	286	**
O III	88	7.2	54	47	$4.4 \times 10^{-5}$
	52	54.0	160	106	
N II	122	0.83	11	10.2	$4.6 \times 10^{-5}$
N III	57	62	165	103	$4.3 \times 10^{-5}$

\*  $14'' \times 20''$ .

\*\* see text

Rubin et al. (1991, 1993) and Osterbrock et al. (1992). Rubin has used far infrared airborne measurements so that  $T_e$  is usually not important. The iron abundance has been considered only by Osterbrock et al. (1992), and is unfortunately poorly determined because the atomic data is uncertain for the transitions they observe.

The C, N and O abundances are very similar to the B star abundances, so that the discussion given above applies here as well. The Ne/Ar ratio is about the same as in NGC 6302, but the abundance of both of these elements to a factor 2 to 3 lower. If Ne has been enriched in the evolution of NGC 6302, then it is likely that Ar has also been enriched. For sulfur and chlorine there is agreement to within a factor 2. Sodium and potassium are an order of magnitude underabundant in the ISM compared to the sun, B stars and NGC 6302. The other elements are clearly underabundant with respect to the Sun and B stars, and are probably in the form of dust. They are also more underabundant in the interstellar medium than in NGC 6302, with the possible exception of iron. Mg and Si are one order of magnitude less abundant, while Ca is a factor 100 less abundant. This probably should be interpreted as a different equilibrium between the gas and dust in the interstellar medium as in NGC 6302. This might have been expected in the cool clouds, whose physical conditions are so different than in NGC 6302. This is not true of the H II region, but the information on these particular elements is so sparse that a comparison cannot yet be made.

## 9. The outer regions of NGC 6302: the LWS measurements

The LWS has measured the spectrum of NGC 6302 from 43 microns through 197 microns (Liu, 1997). The beam of the LWS is much greater than the SWS; about  $80'' \times 80''$  compared to the  $20'' \times 14''$  of the SWS (Burgdorf et al., 1997). Thus the LWS has measured essentially the entire nebula and we cannot directly compare the LWS measurements with the SWS.

We shall analyse the LWS measurements which consist of N II, N III, O I, O III and C II lines, in the following way. From our analysis of the inner regions (the SWS data) we are able to predict the strength of the lines of the first 4 of these ions in the inner region. We subtract this emission from the total observed LWS emission to obtain the intensity in the outer region. The results are shown in Table 5. The first two columns give the ion and the wavelength of the line used (in microns). The third

column gives the strength of this line expected from the inner region on the basis of the observed strength of an optical or ultraviolet transition of the ion. For O I,  $\lambda 6300$  was used; for O III  $\lambda 5007$ , for N II  $\lambda 6584$  and for N III  $\lambda 1750$  was used. In all cases the intensities are given in Paper I. An electron temperature  $T_e = 15\,000$  K was used for O I and N II, while  $T_e = 18\,000$  K was used for O III and N III. This predicted intensity is seen to always be considerably smaller than the total LWS intensity given in Column 4. Column 5 gives the difference between columns 4 and 3, and is the intensity of the line in the outer regions.

It is possible to derive the average electron density  $N_e$  in the outer region from the ratio of the two O III lines. The value obtained is  $N_e = 850$  cm $^{-3}$ , an order of magnitude lower than in the inner region. While it is expected that the density decreases outwardly, there is not sufficient information for a detailed model. It is however possible to estimate the ionic abundances in the outer region. For this one needs to know the  $H\beta$  flux for this region. This is obtained as follows. The 6 cm radio continuum flux density of the entire nebula is 3000 mJy (Rodriguez et al., 1985). For a value of  $T_e = 17\,000$ ,  $He^+/H = 0.11$  and  $He^{++}/H = 0.06$ , an  $H\beta$  flux for the nebula of  $5.6 \times 10^{-10}$  erg cm $^{-2}$  s $^{-1}$  is found. Since the inner region has an  $H\beta$  flux of  $2.4 \times 10^{-10}$  erg cm $^{-2}$  s $^{-1}$  (Paper I), the  $H\beta$  flux of the outer region is  $3.2 \times 10^{-10}$  erg cm $^{-2}$  s $^{-1}$  (no further extinction corrections are necessary). The abundances can now be calculated in the same manner as for the inner region and the results are given in the last column of Table 5.

The abundances may be compared with those of the inner region given in Table 3. For nitrogen it can be seen that N II is 50% higher in the outer region and N III about 50% lower. This indicates that the ionization is somewhat less in the outer region as might be expected. Similarly, O III in the outer region is half what it was in the inner region, but it is expected that O II will be higher. Taken together, there is no reason to expect that the abundance differs from the two regions.

An important conclusion can be drawn from this agreement. The abundances of N II, N III and O III in the inner region were determined from optical and ultraviolet lines and are sensitive to the temperature, and in particular to temperature fluctuations, if they exist. The abundances in the outer region are determined from the far infrared lines, which are not at all sensitive to the precise value of the temperature (or to temperature fluctuations). The good agreement is a confirmation that temperature fluctuations are not important (less than 50%) in determining the ionic abundances.

In Table 5 we have not given an abundance for O I. If it is formed in the same region as the other ions, i.e. the region in which hydrogen is ionized, the abundance can be found in the same way as the other ions. We then find:  $N(O I)/H^+ = 1.6 \times 10^{-4}$ . This is considerably higher than the O III abundance. It is possible that part of the O I line is formed in a neutral hydrogen region, especially since the ionization potential of neutral oxygen and neutral hydrogen are almost the same. The ratio  $N(C II)/N(O I)$  can also be determined, since an intensity of the  $158 \mu m$  line has been measured by the LWS, having  $I = 15 \times 10^{-12}$  erg cm $^{-2}$  s $^{-1}$ . This gives:

$$\frac{N(\text{C II})}{N(\text{O I})} = 1.2 \quad (2)$$

But since it is difficult to say how much of each line has been formed in the ionized or neutral region, this ratio cannot at present be related to the abundances.

## 10. Discussion and conclusions

In this section 5 topics are listed, together with a discussion of the conclusions which can be drawn from the ISO spectra.

### 10.1. Missing stages of ionization

This has always been an important problem in the past. With the present observations, this problem disappears for many elements, since all of the important ionization stages have been measured. This is true of Ne, N, Ar and even Fe and O. One can now reverse the argument, and ask how good the “ionization correction factors” which are given in the literature are. Torres-Peimbert & Peimbert (1997) mention two factors. The first is:

$$\frac{Ne}{O} = \frac{Ne^{++}}{O^{++}} \quad (3)$$

We find (Table 3) that  $Ne/O = 1.1$  and  $Ne^{++}/O^{++} = 0.91$ . This is at first sight reasonably good agreement. But here the  $Ne^{++}$  abundance has been determined from the ISO infrared lines. If the ultraviolet line at  $\lambda 3869$  had been used, as is usual, a much lower  $Ne^{++}$  abundance would have been found. This problem has been discussed in an earlier section.

The second “ionization correction factor” is:

$$\frac{N}{O} = \frac{N^+}{O^+} \quad (4)$$

We find  $N/O = 1.5$  and  $N^+/O^+ = 2.64$ . This is now a difference of almost 80%. It indicates that “ionization correction factors” based on simple arguments about the similarity of ionization potentials should be used with caution.

### 10.2. Temperature fluctuations

This rather old concept has had a renewed attraction in explaining the abundance differences found between what is found from collisionally excited  $C^{++}$  and that found from the recombination line of  $C II$ . The abundances found from the ISO lines are formed from such low lying levels that the temperature dependence is small. We can therefore check if it is necessary to postulate temperature fluctuations. In the inner region it was necessary to use optical and ultraviolet lines to determine O and N abundances, because no ISO lines were available for this small region. For the outer region the abundances of O and N were determined from ISO measurements. The fact that the same abundances were found for the two regions, indicates that it was not necessary to introduce temperature fluctuations.

It was however found that the electron temperature varies as a function of the ionization potential of the observed ion

(see Fig. 1). The ionization potentials below about 50 eV,  $T_e$  decreases from about 22 000 K to about 13 000 K in a uniform manner. This corresponds to a temperature decrease in the outer parts of the inner region.

The abundances presented here are not affected by electron temperature in any important way.

### 10.3. Nebular masses

These masses have not been discussed earlier, but they are implicit in the electron densities given for the different regions. If the distance as given by the expansion method is correct ( $d = 1.6$  Kpc, Gomez et al., 1993) and the density found in earlier sections is uniformly distributed, then the inner region mass (including 40% helium contribution) is:

$$\begin{aligned} R &\simeq 2 \times 10^{17} \text{ cm}, N_e \simeq 1.1 \times 10^4 \text{ cm}^{-3} \\ M &= 5.0 \times 10^{-1} M_{\odot} \end{aligned} \quad (5)$$

That this mass is approximately correct can be checked by computing the  $H\beta$  flux coming from a region of this size and (uniform) density at the above distance. This flux is about 50% less than observed ( $2.4 \times 10^{-10} \text{ erg cm}^{-2} \text{ a}^{-1}$ ), but since the line-of-sight dimension is poorly known, this can be considered to be reasonable agreement.

The same calculation can be done for the outer region. There are two difficulties. The first is that the volume observed by the LWS is probably larger than the actual nebular volume. The second is that the average density  $8.9 \times 10^2 \text{ cm}^{-3}$  is only a very rough approximation, since the actual density must have a steep gradient. If the average density is assumed, and the volume is determined as that which will produce the  $H\beta$  flux, we find a volume of  $1.3 \times 10^{54} \text{ cm}^3$  as the emitting region. This lead to a mass in the outer region of  $1.7 M_{\odot}$ .

In total this is about  $2 M_{\odot}$  in ionized nebular material. To this must be added the neutral and molecular matter that surrounds the nebula, for both neutral hydrogen absorption (Rodriguez et al. 1985) and CO (Huggins & Healy, 1989) have been observed.

### 10.4. Abundances and dust depletions

By comparing the nebular abundances with the sun and B stars, there is convincing evidence that Mg, Al, Ca and Fe are depleted in the gas. Since these same elements are depleted in the interstellar medium, it is likely that it is for the same reason: the elements are in the form of dust. In this connection it is strange that Si is not noticeably depleted, since it is clearly seen as a compound in the dust features observed in the nebular (Waters et al. 1996). But a factor 2 depletion could be present, but not detectable.

There is not enough information to say whether O or C is present in important amounts in the dust. It is expected that the depleted “metals” listed above will be in the form of compounds together with O and/or C. Probably the amounts of the “metals” are too low to significantly affect the O or C abundances, but this is not yet certain.

The dust depletions are substantially lower than the depletions in the cool clouds in the interstellar medium. This is not unexpected, since the conditions are so different. It would be interesting to calculate the equilibrium in detail, but this is beyond the scope of this paper.

### 10.5. Abundances and evolution

The abundances of some of the elements can be used to discuss the nuclear processes which have occurred in the central star. The basis for this is the assumption that the central star, when it was formed, had about the same abundance as the nearby B stars have now. There are clear changes.

Helium is now about 70% overabundant, presumably converted H dredged up and expelled. The C, N and O abundances are much different than in B stars, although the sum of the 3 elements is about the same. This argues that conversion of both C and O into N has occurred: carbon is a factor of 3 underabundant with respect to the B stars, and O a factor 2. While the error on the oxygen abundance could be enough to bring this conclusion into question, it is unlikely that enough C could have been converted to explain the rather large nitrogen to oxygen ratio.

The neon, and possibly argon, abundances are high with respect to B stars. This points to the production of Ne in the course of evolution, which has already been discussed in the literature. Argon, however, is thought not to have undergone nuclear processes. However the evidence from the nebular abundances is quite strong: argon is almost as abundant as sulfur in the nebula, while it is an order of magnitude lower in both the sun and the ISM cool clouds.

*Acknowledgements.* We thank Dr. M. Perinotto for his careful reading of the manuscript and his suggestions for clarifying the text.

### References

- Aller L.H., Ross J.E., O'Mara B.J., Keyes C.D., 1981, MNRAS 197, 95  
 Aller L.H., 1994, ApJ 432, 427  
 Anders E., Grevesse N., 1989, Geochim. Cosmo. 53, 197  
 Barral J.F., Canto J., Meaburn J., Walsh J.R., 1982, MNRAS 199, 817  
 Beintema D.A., Pottasch S.R., 1999, A&A (Paper I)  
 Burgdorf M., Clegg P., Ewart D., et al., 1997, ISO Workshop ESA SP-419, p. 51  
 Butler K., Zeippen C.J., 1994, A&AS 108, 1  
 Gies D.R., Lambert D.L., 1992, ApJ 387, 673  
 Grevesse N., Noels A., 1993, In: Prantos N., et al. (eds.) Origin of the Elements. Cambridge University Press, p. 15  
 Gomez Y., Rodriguez L.F., Moran J.M., 1993, ApJ 416, 620  
 Huggins P.J., Healy A.P., 1989, ApJ 346, 201  
 Killian-Montenbruck J., Gehren T., Nissen P.E., 1994, ApJ 291, 757  
 Liu X.-W., 1997, ISO Workshop ESA SP-419, p. 87  
 Mendoza C., 1983, In: Flower D.R. (ed.) IAU Symp. 103, Planetary Nebulae. p. 143  
 Oliva E., Pasquali A., Reconditi M., 1996, A&A 305, L21  
 Osterbrock D.E., Tran H.D., Veilleux S., 1992, ApJ 389, 196  
 Pottasch S.R., 1997, In: Habing H.J., Lamers H.J. (eds.) IAU Symp. 180, Planetary Nebulae. p. 483  
 Rodriguez L.F., Garcia-Barreto J.A., Canto J., et al., 1985, MNRAS 215, 353  
 Rubin R.H., Simpson J.P., Haas M.R., Erickson E.F., 1991, ApJ 374  
 Rubin R.H., Dufour R.J., Walter D.K., 1993, ApJ 413, 237  
 Savage B.D., Sembach K., 1996, A&AR 34, 279  
 Terzian Y., 1997, In: Habing H.J., Lamers H.J. (eds.) IAU Symp. 180, Planetary Nebulae. p. 29  
 Torres-Peimbert S., Peimbert M., 1997, In: Habing H.J., Lamers H.J. (eds.) IAU Symp. 180, Planetary Nebulae. p. 175  
 Waters L.B.F.M., Molster F.J., de Jong T., et al., 1996, A&A 315, L361